Defect and Diffusion Forum
ISSN: 1662-9507, Vol. 452, pp 27-31
doi:10.4028/p-QD8ybH

Submitted: 2025-09-12
Revised: 2026-01-10
Accepted: 2026-02-23
Online: 2026-05-18

Influence of Temperature Field and Doping on BPD Distribution in 8-Inch 4H-SiC Substrates

Z. X. Fu[1,a], X. L. Yang[1,b*], X. F. Chen[1,c*], X. J. Xie[1,d], L. Sun[1,e], H. Y. Shao[1,f], W. H. Han[1,g], H. X. Wang[1,h], G. J. Yu[2,i], X. G. Xu[1,j]

[1]State Key Laboratory of Crystal Materials, Institute of Novel Semiconductors, Shandong University, Jinan, 250100, China

[2]Guangzhou Summit Crystal Semiconductor Co., Ltd, Guangzhou, 511462, China

[a]fuzhenxing1122@126.com, [b]yangxl2016@sdu.edu.cn, [c]cxf@sdu.edu.cn, [d]xiexj@sdu.edu.cn, [e]sdusunli@sdu.edu.cn, [f]202114048@mail.sdu.edu.cn, [g]hwh@mail.sdu.edu.cn, [h]202434144@mail.sdu.edu.cn, [i]YuGuojian@summitcrystal.com, [j]xxu@sdu.edu.cn

Keywords: 4H-SiC, 8-inch, BPD distribution, dislocations slip.

Abstract. 8-inch 4H-SiC single crystals were grown under different temperature fields and nitrogen doping conditions by physical vapor transport method. The distributions of basal plane dislocation (BPD) in 4H-SiC single crystals under different growth conditions were studied by molten KOH etching and X-ray Topography (XRT). The results indicate that the BPDs in the crystals grown under convex temperature field are distributed at the edge. In comparison, the BPD distributions in crystals grown under a concave temperature field are relatively closer to the center. Furthermore, the BPDs distributions in nitrogen-doped crystals exhibit quadratic symmetry caused by prismatic slip. In contrast, no prismatic slip-induced slip bands were observed in the undoped crystals, and the BPD distributions in the undoped crystals are consistent with the shear stress distribution caused by basal plane slip.

Introduction

As a representative of the third-generation semiconductors, silicon carbide (SiC) exhibits excellent physical and chemical properties, offering a wide range of research and application scenarios [1,2]. Dislocation is one of the main factors limiting crystal quality, among which BPDs could lead to positive voltage drift during device operation. Due to the large size of 8-inch 4H-SiC crystals, it is difficult to control the temperature field [3,4]. During the growth process of 8-inch crystals under different temperature fields, the distribution of thermal stress varies, which leads to differences in the distribution of BPDs within the crystal. In addition, nitrogen doping, as a method to adjust the resistivity of SiC crystals to adapt to different needs, changes the physical properties of SiC by replacing carbon atoms with nitrogen atoms[5]. Since the diameter of nitrogen atoms is smaller than that of carbon atoms, the occupation of carbon sites by nitrogen atoms affects lattice matching[6]. Nitrogen doping is found to facilitate the nucleation of BPDs and decrease the shear stress required for the nucleation of BPDs [7].

In this work, we grown 4H-SiC single crystals under different temperature fields and nitrogen doping conditions using the physical vapor transport (PVT) method. The distribution characteristics of BPD in the crystals under different conditions were studied through molten KOH etching and XRT.

Experiments

8-inch 4H-SiC single crystals were grown on seeds with 4° off-angle using the PVT method. The growth temperature of the crystals was maintained at 2000~2200°C, and the growth pressure was set at 1~10 mbar. Other growth conditions are as shown in the Table 1, with the temperature field and whether nitrogen is doped as variables.

Table 1. Growth Conditions of Different Crystals.

Grown crystals	Temperature fields	Doping
Crystal A	Convex	N-doped
Crystal B	Concave	N-doped
Crystal C	Convex	undoped

Wafers from the early growth stage of these crystals were selected and etched by molten KOH solution at 500°C for 30 minutes. These wafers were labeled as Wafer A1, B1, and C1, respectively. The dislocation morphology of the etched samples was observed using an optical microscope. Adjacent wafers to the etched ones were observed by XRT with the diffraction vector g=11-20, which were labeled as Wafer A2, B2, and C2.

Results and Discussion

The BPD distributions of crystals grown in different temperature fields and nitrogen doping conditions are shown in Fig. 1. The BPDs in Wafer A1 are distributed at the edges, while the BPDs in Wafer B1 are away from the edges and more closely distributed towards the center. The reason is that the thermal stress generated during crystal growth under a convex temperature field is mainly distributed at the edges, whereas under a concave temperature field, the stress near the center of the crystal increases compared to the convex temperature field, leading to a distribution of BPDs closer to the center.

The BPD distribution of Wafer C1 is shown in Fig. 1(c). The BPDs in Wafer C1 are also distributed at the edges similar to that in Wafer A. The difference is that the positions with the highest BPD density in Wafer C1 are at the ends of a straight line parallel to the [1-100] direction and passing through the center of the wafer. However, the positions with the highest BPD density in Wafer A1 are four other areas, which is consistent with the report by Lu et al [8]. Although Crystal B was grown under a different temperature field, the distribution of BPDs in wafer B1 also exhibits the same fourfold symmetry as in Wafer A1. This result indicates that nitrogen doping affects the distribution of BPDs in 4H-SiC.

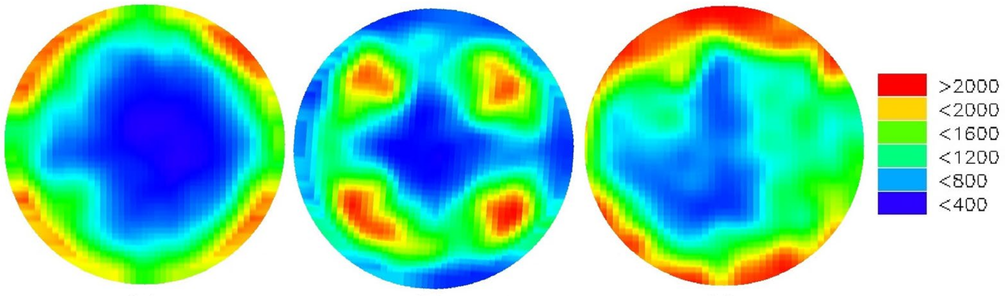

(a) (b) (c)

Fig. 1. BPD density distribution map of (a) Wafer A1, (b) Wafer B1 and (c) Wafer C1.

After etching, 12 areas on Wafer A1 were observed, and the results are shown in Fig. 2(a). The BPD directions at different locations exhibit a certain pattern: in each area, the BPD etch pits mainly have two directions, both of which are two out of [11-20], [1-210] and [-2110]. The distribution characteristics of the BPD directions show a 12-fold symmetry, similar to the pattern discovered by Hu et al [9]. Additionally, among the four high dislocation density locations corresponding to Fig. 1(a), the number of BPDs along the [11-20] direction is significantly higher than that along other directions. This indicates that the reason for the fourfold symmetry in BPD density distribution is due to an increase in the number of BPDs in the [11-20] direction at specific locations.

Lu et al. [10] have pointed out that the primary dislocation slip mode during the growth of 8-inch 4H-SiC crystals is prism slip. By observing 12 areas on Wafer A2 using XRT, as shown in Fig. 2(b), a large number of dislocation lines caused by prism slip were found in the 12 areas of Wafer A2, and the direction of these dislocation lines is consistent with the direction of BPD etch pits at the same positions in Wafer A1. Furthermore, a greater number of prism dislocation lines [11] were observed in the four positions with the highest BPD density. This indicates that in N-doped 4H-SiC crystals grown under convex temperature fields, prism slip is the main cause of BPD generation.

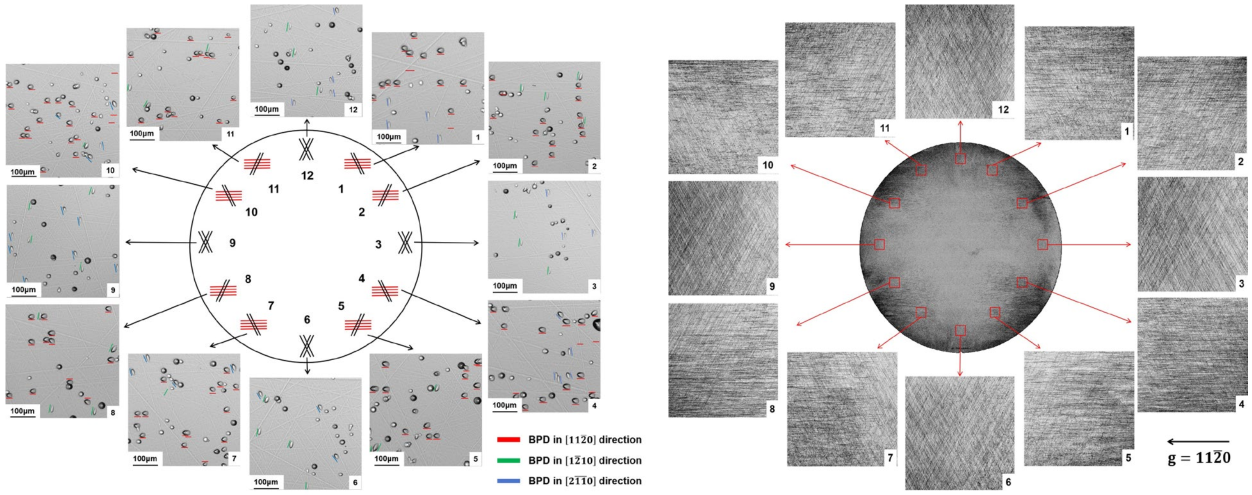

(a) (b)

Fig. 2. (a) Morphology of BPD etch pitson Wafer A1, (b) Prismatic dislocations on Wafer A2.

Fig. 3(a) shows the optical microscope images of BPD etch pits in 12 areas of Wafer B1, with the selected 12 positions being closer to the center of the wafer. The BPDs direction in Wafer B1 exhibit a 12-fold symmetric distribution, and the BPD quantities show a fourfold symmetric distribution, same as those in Wafer A1. Moreover, the number of BPDs in the [11-20] direction is higher than others. Fig. 3(b) presents the XRT image of Wafer B2, where the distribution of prism dislocations are highly consistent with those of BPD. This indicates that in N-doped 4H-SiC crystals grown under concave temperature fields, the main cause of BPD generation is still prism slip.

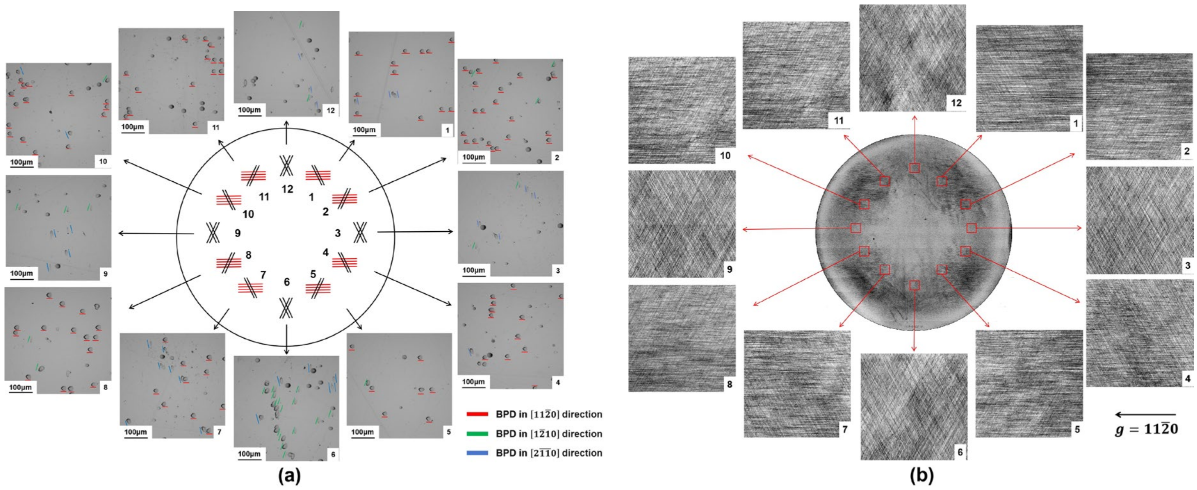

Fig. 3. (a) Morphology of BPD etch pits on Wafer B1, (b) Prismatic dislocations on Wafer B2.

Fig. 4(a) shows the BPD etch pit images in 12 areas of Wafer C1, with the selected 12 areas being the same as those in wafer A1. The characteristics of BPD in Wafer C1 are completely different from the patterns observed in wafers A1 and B1. The directions of BPD etch pits in Wafer C1 are random. Fig. 4(b) presents the XRT image of 12 areas in Wafer C2, where no prism dislocation lines were observed. This indicates that in undoped 4H-SiC crystals grown under convex temperature fields, prism slip has no contribution to the generation of BPD. Moreover, the BPD distribution shown in Fig. 1(c) is consistent with the results of basal plane slip reported by Lu et al., suggesting that in undoped 4H-SiC crystals, basal plane slip is the main cause of BPD generation.

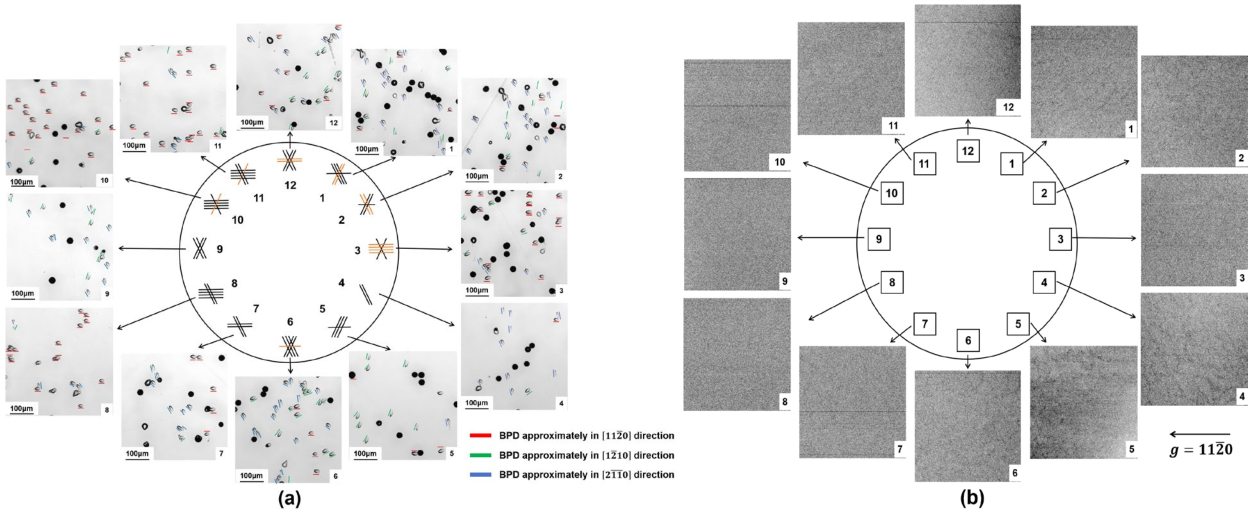

Fig. 4. (a) Morphology of BPD etch pits on Wafer C1, (b) Prismatic dislocations on Wafer C2.

Crystals A and C grow under the same temperature field, but the causes of BPD generation are different. Nitrogen doping is the reason for this phenomenon. It is well known that the {0001} face is the close-packed surface of 4H-SiC, so basal plane slip occurs more easily than prism slip. Therefore, in crystal C, basal plane slip plays a dominant role in the generation of BPD. After nitrogen doping, the critical shear stress of the crystal decreases, leading to the occurrence of prism slip in crystal A, which then dominates, resulting in new characteristics in the BPD distribution.

Summary

Three crystals were grown under different temperature fields and nitrogen doping conditions, and the characteristics of BPD distribution were observed. In the convex temperature field, the BPD is mainly distributed at the edge of the crystal; while in the concave temperature field, the BPD distribution is closer to the center of the crystal, which is related to the stress distribution under different temperature fields. The BPD distribution in nitrogen-doped crystals shows fourfold symmetry in quantity and twelvefold symmetry in direction, which is related to prism slip; the BPD distribution in undoped crystals shows axial symmetry in quantity and no regularity in direction, which is related to basal plane slip.

Acknowledgement

This work was supported by the National Natural Science Foundation of China (Grant No. U23A20569), the Key R&D Program of Shandong Province (2022ZLGX02) and the Taishan Scholars Program.

References

[1] X. X. Xiong, X. L. Yang, X. F. Chen, X. M. Li, X. J. Xie, G. J. Hu, Y. Peng, G. J. Yu, X. B. Hu, Y. H. Wang, X. X. Xu, J. Inorg. Mater. 38 (2023) 1371.

[2] Musolino M, Xu X, Wang H, Rengarajan V, Zwieback I, Ruland G, Crippa D, Mauceri M, Calabretta M and Messina, Mater. Sci. Semicond. Process. 135 (2021) 106088.

[3] G. J. Hu, G. L. Zhong, X. X. Xiong, H. D. Li, H. Y. Shao, L. B. Zhao, X. M. Li, X. L. Yang, X. F. Chen, X. J. Xie, Y Peng, G. J. Yu , X. B. Hu, X. G. Xu, Vacuum 222 (2024) 112961.

[4] S. T. Zhang, G. Q. Fu, H. D. Cai, J. Z. Yang, G. F. Fan, Y. Y. Chen, T. Li and L. L. Zhao, Materials 16 (2023) 767.

[5] Y. X Cui, X. B. Hu, K. Yang, X. L. Yang, X. J. Xie, L. F. Xiao and X. G. Xu, Cryst. Growth Des. 15 (2015) 3131−3136.

[6] H. D. Li, X. L. Yang, X. C. Jiang, H. Y. Shao, G. J. Hu, X. M. Li, Y. Peng, X. F. Chen, X. B. Hu, X. J. Xie, G. J. Yu and X.G. Xu. Phys. Scr. 99 (2024) 0959a6.

[7] B. Kallinger, P. Berwian, J.Friedrich, G. Müller, A. D. Webe, E. Volz, G. Trachta, E. Spiecker, B. Thomas, J. CRYST. GROWTH. 349 (2012) 43-49.

[8] X. S. Liu, R. Wang, J. R. Zhang, Y. H. Lu, Y. Q. Zhang, D. R. Yang and X. D. Pi, J. Phys. D: Appl. Phys. 55 (2022) 334002.

[9] S. O Lu, B. J Xu, Y. Z. Wang, H. Y. Chen, W. Hang, R. Wang, J. L. Yuan, X. D. Pi, D. R. Yang and X. F. Han, CrystEngComm. 26 (2024) 2143.

[10] S. S. Hu, S. Fang, Y. F. Liu, Q.Y. Cheng, H. Y. Peng, Z. Y. Chen, Y. H. Gao, C. Gao, B.Raghothamachar and M. Dudley, Mater. Sci. Forum, 1089 (2023) 45-50.

[11] S. O. Lu, B. J. Xu, L. L. Xuan, X. D. Pi, D. Yang and X. F Han, CrystEngComm, 26 (2024) 6244.

[12] J.Q. Guo, Y. Yang, B. Raghothamachar, J. Kim, M. Dudley, G. Chung, E. Sanchez, J. Quas and I. Manning, J, Electron. Mater. 46 (2017) 2040.